

See discussions, stats, and author profiles for this publication at: <https://www.researchgate.net/publication/266670816>

# A Variational Approach to the Numerical Simulation of Hydraulic Fracturing

Conference Paper · October 2012

DOI: 10.2118/159154-MS

CITATIONS

151

READS

428

3 authors, including:



**Chukwudi Chukwudozie**  
Columbia University

10 PUBLICATIONS 463 CITATIONS

[SEE PROFILE](#)



**Keita Yoshioka**  
Montanuniversität Leoben

81 PUBLICATIONS 1,193 CITATIONS

[SEE PROFILE](#)

# A Variational Approach to the Numerical Simulation of Complex Hydraulic Fracturing

Blaise Bourdin, Department of Mathematics and Center for Computation & Technology, Louisiana State University  
 Chukwudi Chukwudozie, Craft & Hawkins Department of Petroleum Engineering, Louisiana State University  
 Keita Yoshioka, Chevron Energy Technology Company.

## Abstract

One of the most critical capabilities of realistic hydraulic fracture simulation is the prediction of complex (turning, bifurcating, or merging) fracture paths. In most classical models, complex fracture simulation is difficult due to the need for a priori knowledge of propagation path and initiation points and the complexity associated with stress singularities at fracture tips.

In this study, we follow Francfort and Marigo's variational approach to fracture, which we extend to account for hydraulic stimulation. We recast Griffith's criteria into a global minimization principle, while preserving its essence, the concept of energy restitution between surface and bulk terms. More precisely, to any admissible crack geometry and kinematically admissible displacement field, we associate a total energy given as the sum of the elastic and surface energies. In a quasi-static setting, the reservoir state is then given as the solution of a sequence of unilateral minimizations of this total energy with respect to any admissible crack path and displacement field. The strength of this approach is to provide a rigorous and unified framework accounting for new cracks nucleation, existing cracks activation, and full crack path determination (including complex behavior such as crack branching, kinking, and interaction between multiple cracks) without any a priori knowledge or hypothesis.

Of course, the lack of a priori hypothesis on cracks geometry is at the cost of numerical complexity. We present a regularized phase field approach where fractures are represented by a smooth function. This approach makes handling large and complex fracture networks very simple yet discrete fracture properties such as crack aperture can be recovered from the phase field. We compare variational fracture simulation results against several analytical solutions and also demonstrate the approach's ability to predict complex fracture systems with example of multiple interacting fractures.

## 1. Introduction

Conventionally, in most numerical modeling strategy of hydraulic fracturing, fracture propagation is assumed to be planar and perpendicular to the minimum reservoir stress [1], which simplifies fracture propagation criteria to mode-I and aligns the propagation plane to the simulation grid. Restricting propagation mode search into one direction and prescribing fracture growth plane can greatly reduce computation overhead and make practical numerical modeling tractable. However, recent observations suggest creation of nonplanar complex fracture system during reservoir stimulation [18] or waste injection [19]. To address predictive capabilities of complex fracture propagation, several different approaches, namely, mixed-mode fracture growth criterion with a single fracture [21], multiple discrete fractures that grow with empirical correlations [16], and implicit fracture treatment with the idea of stimulated reservoir volume where averaged properties are estimated over an effective volume [17] have been proposed. In this study, we propose to apply the variational approach to fracture [10, 15] to hydraulic fracturing. One of the strengths of this approach is to account for arbitrary numbers of pre-existing or propagating cracks in terms of energy minimization, without any a priori assumption on their geometry, and without restricting their growth to specific grid directions.

The goal of this paper is to present early results obtained with this method. At this stage, we are not trying to account for all physical, chemical, thermal, and mechanical phenomena involved in the hydraulic fracture process. Instead, we propose a mechanistically sound yet mathematically rigorous model in an ideal

albeit not unrealistic situation, for which we can perform rigorous analysis and quantitative comparison with analytical solutions. In particular, we neglect all thermal and chemical effects, we assume that the injection rate is slow enough that all inertial effects can be neglected, and place ourself in the quasi-static setting. Furthermore, we consider a reservoir made of an idealized impermeable perfectly brittle linear material with no porosity and assume that the injected fluid is incompressible. These assumptions imply that no leak-off can take place and that the fluid pressure is constant throughout the fracture system (infinite fracture conductivity), depending only on total injected fluid volume and total cracks opening respectively. Also, throughout the analyses presented, we only deal with dimensionless parameters, which are normalized by the Young's moduli for mechanical parameters and by the total domain volume for volumetric parameters.

## 2. The variational approach to hydraulic fracturing

In classical approaches to quasi-static brittle fracture, the elastic energy restitution rate,  $G$ , induced by the infinitesimal growth of a single crack along an a priori known path (derived from the stress intensity factors) is compared to a critical energy rate  $G_c$  and propagation occurs when  $G = G_c$ , the celebrated Griffith criterion. The premise of the variational approach to fracture is to recast Griffith's criterion in a variational setting, *i.e.* as the minimization over any crack set (any set of curves in 2D or of surface in 3D, in the reference configuration) and any kinematically admissible displacement field  $u$ , of a total energy consisting of the sum of the stored potential elastic energy and a surface energy proportional to the length of the cracks in 2D or their area in 3D.

More specifically, consider a domain  $\Omega$  in 2 or 3 space dimension, occupied by a perfectly brittle linear material with Hooke's law  $\mathbf{A}$  and critical energy release rate (also often referred to as fracture toughness)  $G_c$ . Let  $f(t, x)$  denote a time-dependent<sup>1</sup> body force applied to  $\Omega$ ,  $\tau(t, x)$ , the surface force applied to a part  $\partial_N \Omega$  of its boundary, and  $g(t, x)$  a prescribed boundary displacement on the remaining part  $\partial_D \Omega$ . To any arbitrary crack set  $\Gamma$  and any kinematically admissible displacement set  $u$ , we associate the total energy

$$F(u, \Gamma) := \int_{\Omega \setminus \Gamma} W(e(u)) \, d\Omega - \int_{\partial_N \Omega} \tau \cdot u \, ds - \int_{\Omega} f \cdot u \, d\Omega + G_c \mathcal{H}^{N-1}(\Gamma), \quad (1)$$

where  $f$  and  $\tau$  denote surface and body forces applied to  $\Omega$ ,  $W$  is the elastic energy density associated with a linearized strain field  $e(u) := (\nabla u + \nabla^T u)/2$ , given by  $W(e(u)) := \mathbf{A}e(u) : e(u)$ , and  $\mathcal{H}^{N-1}(\Gamma)$  denotes the  $N - 1$ -dimensional Hausdorff measure of  $\Gamma$ , *i.e.* the length of  $\Gamma$  in two space dimensions and its surface area in three space dimensions.

In the setting of variational fracture, the criticality of the elastic energy release rate is replaced with unilateral minimality of the total energy  $F$  with respect to *any* admissible displacement field  $u$  and *any* crack set satisfying a crack growth condition. More specifically, at any discrete time step  $t_i$ , we look for the solution  $(u_i, \Gamma_i)$  of the minimization problem:

$$\inf_{\left\{ \begin{array}{l} u \text{ kinematically admissible} \\ \Gamma \subset \Gamma_j \text{ for all } j < i \end{array} \right\}} F(u, \Gamma). \quad (2)$$

Loosely speaking, minimality with respect to the displacement field accounts for the fact that the system achieves static equilibrium under its given crack set, optimality with respect to the crack set is a generalization of Griffith's stationarity principle  $G = G_c$ , and the growth constraint  $\Gamma \subset \Gamma_j$  for any  $j < i$  accounts for the irreversible nature of the fracture process.

---

<sup>1</sup>We follow a common abuse of language by referring to  $t$  as "time". Rigorously, as we place ourselves in the context of quasi-static evolution,  $t$  is to be understood as an increasing loading parameter.

We insist that in (2), no assumption is made on the geometry of the crack set, other than the growth condition. In particular, one does not even assume that  $\Gamma$  consists of a single crack curve or surface, or that the number of cracks remains constant during the evolution (which would preclude nucleation or merging). Indeed, one strength of the variational approach is *to provide a unified setting for the path determination, nucleation, activation and growth of an arbitrary number of cracks in two and three space dimensions*.

The numerical implementation of (2) is a challenging problem that requires carefully tailored techniques. The admissible displacement fields are discontinuous, but the location of their discontinuities is not known in advance, a requirement of many classical discretization methods. Also, the surface energy term in (1) requires approximating the location of cracks, together with their length, a much more challenging issue (see the studies of anisotropy induced by the grid [12] and the mesh [20]).

The approach we present here is based on the variational approximation by elliptic functionals [2, 3]. A small regularization parameter  $\varepsilon$  is introduced and the location of the crack is represented by a smooth “phase field function”  $v$  taking values 0 close to the crack and 1 far from them. More precisely, one can prove (see [11, 13, 14] for instance) that as  $\varepsilon$  approaches 0, the regularized energy

$$F_\varepsilon(u, v) := \int_{\Omega} v^2 W(e(u)) \, d\Omega - \int_{\partial_N \Omega} \tau \cdot u \, ds - \int_{\Omega} f \cdot u \, d\Omega + \frac{G_c}{2} \int_{\Omega} \frac{(1-v)^2}{\varepsilon} + \varepsilon |\nabla v|^2 \, d\Omega. \quad (3)$$

approaches  $F$  in the sense of  $\Gamma$ -converges, which implies that the minimizers of  $F_\varepsilon$  converge as to that of  $F$ .

The main feature of the regularized problem is that it does not require an explicit representation of the crack network. Instead all computations are carried out on a fixed mesh and the arguments of  $F_\varepsilon$  are smooth functions which can be approached using standard finite elements. Moreover, provided that the discretization size and regularization parameter satisfy some compatibility properties, it can be shown that the  $\Gamma$ -convergence property can be extended to the finite element discretization of  $F_\varepsilon$ . The actual minimization follows the approach originally devised in [7–9] is then achieved by alternating minimization with respect to the  $u$  and  $v$  field, until convergence. Numerical implementation is carried out on parallel supercomputers and is based on the PETSc toolkit [4–6].

### 2.1. Variational approach to hydraulic fracturing

In order to adapt the variational fracture framework to hydraulic fracturing, one has to account for fluid pressure forces along the crack surfaces. For any point  $x$  on the crack set  $\Gamma$ , we denote by  $\nu_\Gamma(x)$  the oriented normal direction to  $\Gamma$  and by  $u^+(x)$  and  $u^-(x)$  the traces of the displacement field. With these notations, the work of the pressure force  $p$  becomes then

$$\int_{\Gamma} p(x) (u^+(x) - u^-(x)) \cdot \nu_\Gamma(x) \, ds,$$

and the total energy becomes

$$E(u, \Gamma) := F(u, \Gamma) + \int_{\Gamma} p(x) (u^+(x) - u^-(x)) \cdot \nu_\Gamma(x) \, ds. \quad (4)$$

Accounting for pressure forces in the regularized formulation is more subtle as the crack geometry is not tracked explicitly, but represented by the smooth field  $v$ . In the sequel, we propose to modify the regularized energy (3) and consider

$$E_\varepsilon(u, v) = F_\varepsilon(u, v) + \int_{\Omega} p(x) u(x) \cdot \nabla v(x) \, d\Omega. \quad (5)$$

Following the lines of the analysis carried out in [13, 14], it can be proven that the  $\Gamma$ -convergence property is preserved so that again, the minimizers of (5) converge to that of (4). Intuitively, surface forces along the edges of  $\Gamma$  are replaced with properly scaled body forces applied in a neighborhood of the cracks.

$h$	1.E-2	6.7E-3	5.7E-3	5.0E-3
Crack volume	2.40E-06	2.47E-06	2.49E-06	2.51E-06

Table 1: Total computed crack volume.

In the next sections, we illustrate some of the properties of this approximation and its ability to properly account for pressure forces and deal with unknown crack path, multiple cracks and changes in the cracks topology.

### 3. Application to a straight crack in 2d.

#### 3.1. Static case: computation of the crack opening displacement:

We first focus on a classical two dimensional static case in plane stress: we consider an infinite domain filled with a homogeneous isotropic material with Young's modulus  $E$  and Poisson ratio  $\nu$  with a single pre-existing crack  $\Gamma$  of length  $2\ell_0$  in the  $y = 0$  plane. Assuming that the displacement and stress fields vanish at infinity, it is then possible to derive an exact formula for the boundary displacement of the crack surface subject to a constant pressure force (see [22, Sec 2.4], for instance). Setting  $E' = E/(1 - \nu^2)$ , we have that for  $-\ell_0 \leq x \leq \ell_0$

$$u^+(x, 0) = \frac{2p\ell_0}{E'} \left(1 - \frac{x^2}{\ell_0^2}\right)^{1/2}, \quad (6)$$

and that  $u^-(x, 0) = -u^+(x, 0)$ . From this, it is easy to derive that the total volume of the crack in the deformed configuration is

$$V = \frac{2\pi p\ell_0^2}{E'}. \quad (7)$$

In order to compare the analytical expression of the crack opening displacement, we built a  $v$  field corresponding to the problem above, then minimized the total energy with respect to the displacement field. Following [10, Sec. 8.1.1], we reproduced the optimal profile constructed for the recovery sequence of  $\Gamma$ -convergence:

$$v_\varepsilon(x, y) = 1 - e^{-d_\Gamma(x, y)/\varepsilon}, \quad (8)$$

where  $d_\Gamma(x, y)$  denotes the distance from a point of coordinate  $(x, y)$  to  $\Gamma$ . From the  $\Gamma$ -convergence construction, it is also possible to see that for any  $-\ell_0 \leq x \leq \ell_0$ , the crack opening displacement is given by

$$\int_{-\infty}^{\infty} u(x, y) \cdot \nabla v(x, y) dy. \quad (9)$$

We ran a series of experiments for a crack of length  $2\ell_0 = .4$  centered in a finite square domain of size  $4 \times 4$  with unit Young's modulus and fracture toughness. The size of  $\Omega$  was chosen so that the choice of boundary condition on  $\partial\Omega$  has no practical impact on the displacement field near the crack. Figure 1 represents the crack opening displacement obtained by (9) after minimization (plain lines) and compared with expression (6) (dashed line) for an injected fluid pressure of 1E-3. We performed computations for mesh sizes  $h$  ranging from 1E-2 to 5E-3, keeping  $\varepsilon$  equal to 1E-2. We observe a slight discrepancy near the crack tips (mostly due to softening effect induced by the smooth crack field  $v$ ), but away from the crack tip, the approximation of the opening displacement is very good, and insensitive to changes of the mesh size. Table 1 presents the computed total crack volume. The theoretical value obtained from (6) is 2.513E-6.

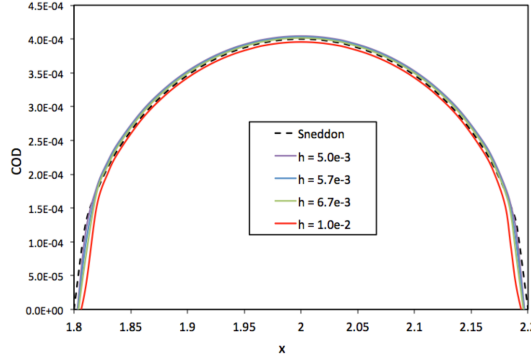


Figure 1: Crack opening displacement obtained by applying (9) to a synthetical  $v$  field compared to the analytical solution.

### 3.2. Propagation under prescribed injected volume:

We then focused on the quasi-static crack evolution in this situation. In this situation, the elastic energy release rate can easily be derived from the crack opening displacement (6), and the quasi-static evolution following Griffith criterion obtained. From this analysis, one can see that if the pressure exceed the critical value  $p_0 := \sqrt{\frac{G_c E'}{\pi \ell_0}}$  corresponding to an injected volume  $V_0 := \sqrt{\frac{4\pi G_c \ell_0^3}{E'}}$ , then stable crack propagation becomes impossible. If one prescribes the injected volume  $V$ , however, it is easy to see that below the critical volume  $V_0$ , the crack does not grow, and the pressure grows linearly until it reaches the critical pressure  $p_0$ . For  $V > V_0$ , the crack growth is accompanied by a pressure drop. The pressure and crack length are given by:

$$p(V) = \left[ \frac{2E'G_c}{\pi V} \right]^{1/3}, \quad (10)$$

and

$$\ell(V) = \left[ \frac{E'V^2}{4\pi G_c} \right]^{1/3}. \quad (11)$$

Figures 2, illustrate the effect of the regularization parameter  $\varepsilon$ . We consider a square  $(0, 8) \times (0, 8)$  with a horizontal crack of length .4 in its center, and discretized by a single layer of  $355 \times 355$  bilinear finite elements of size  $h=2.25E-2$  and thickness  $1E-2$ . All components of the displacements are forced to 0 along the boundary of the domain. One observes that as expected, the crack geometry is represented by a smooth function  $v$  taking values near 0 close to crack and gradually increasing to 1 away from the crack. The thickness of the transition zone from 0 to 1 is given by the regularization parameter  $\varepsilon$ , and in the limit of  $\varepsilon \rightarrow 0$ , the  $v$ -field becomes sharper. The profile of the  $v$  field along a cross section through  $x = 0$  for the same value of  $h$  and various values of  $\varepsilon$  is shown in Figure 3. We observe that if  $\varepsilon$  is “too small” compared to the mesh size, the smooth profile is poorly approximated. This is consistent with the compatibility condition for the  $\Gamma$ -convergence of the discretized regularized energy which requires that  $h \ll \varepsilon$ .

Finally, Figure 4 compares the crack pressure and length as a function of the injected volume obtained for the same parameters as above with the closed form expressions (10) and (11). When  $\varepsilon$  is “too large”, the critical pressure is underestimated and the critical volume overestimated. As the crack starts propagating, the computed length and pressures are very close to the exact expression. This behavior is explained by the softening taking place in the transition layer near the crack which reduces the stresses near the crack tip. When  $\varepsilon$  is “too small”, compared to the mesh size, the transition profile is poorly approximated, which leads to a poor approximation of the surface energy, hence of the crack length and pressure.

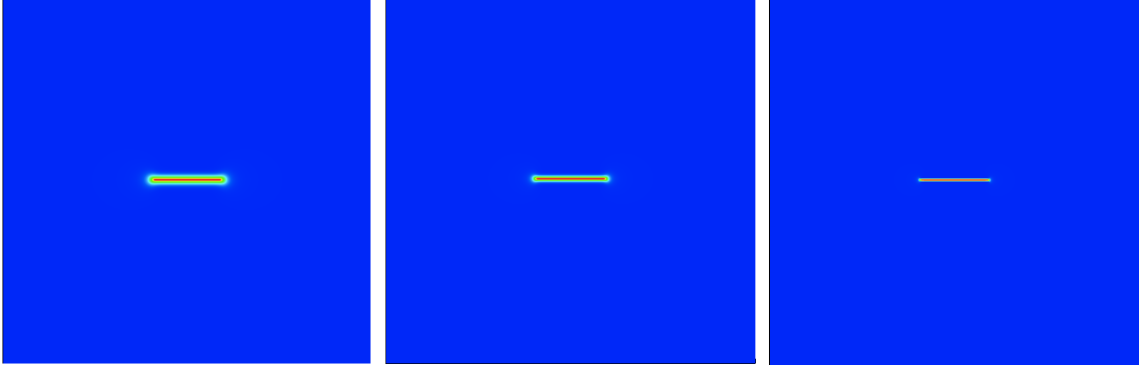


Figure 2: The  $v$  field associated with an injected volume of 2.5 the blue color corresponds to the value 1 (the untracked material) and the red to 0 (the crack). The value of the regularization parameter  $\varepsilon$  is (left to right)  $5.E-3$  ( $2.5h$ ),  $3E-3$  ( $1.5h$ ), and  $5E-2$  ( $.25h$ ). Qualitatively, one observes that the  $v$  field is a smooth function but becomes sharper as  $\varepsilon$  decreases.

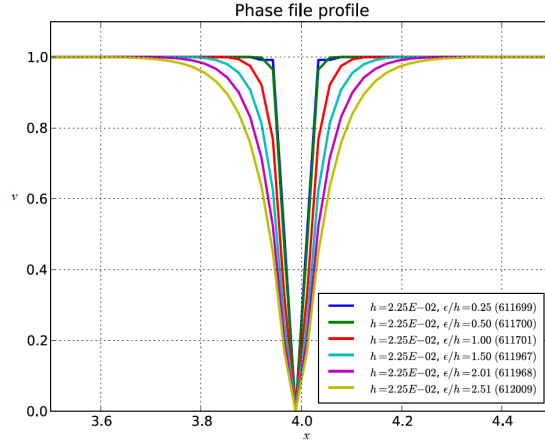


Figure 3: Profile of the  $v$  field along the vertical cross section  $x = 4$ .

In Figure 5, we fixed the ratio  $\varepsilon/h$  and refined the mesh. Again, we observe that the approach is very robust in that the mesh size has almost no influence on the numerical solution. The pressure is slightly overestimated as the crack grows, which is expected given the choice of boundary condition. Conversely, we ran another series of experiments (not shown here) leaving the boundary of the computational domain stress free, which lead to slightly underestimating the pressure, as expected. The approximation of the crack length shows very little sensitivity to the mesh size, and is very close to the expected value.

#### 4. Propagation of a penny shape crack in 3d.

The same analysis can be carried out in three space dimension in which case, the critical pressures and injected volume associated with a pre-existing penny shape crack of radius  $R_0$  are

$$p_0 = \left[ \frac{E' G_c \pi}{4 R_0} \right]^{1/2}, \quad (12)$$

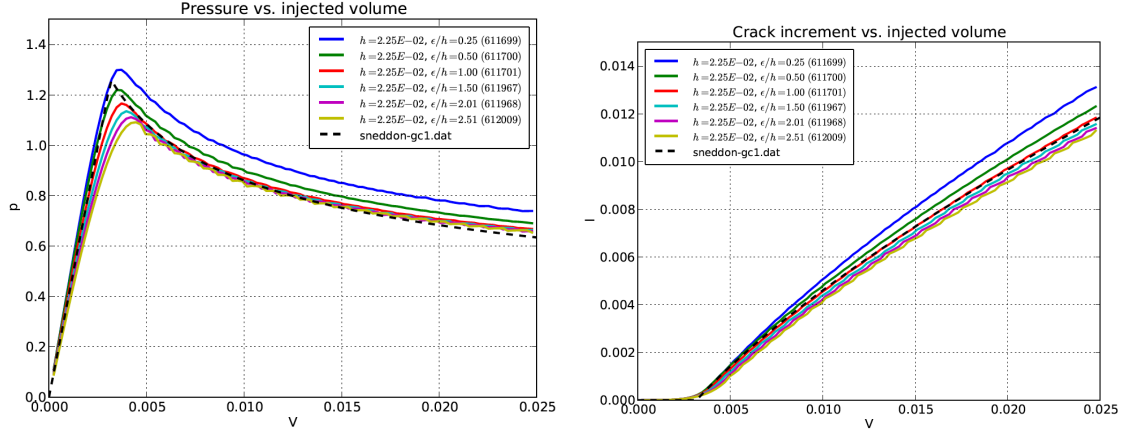


Figure 4: Pressure and length as a function of the injected volume. The solid lines correspond to different values of the regularization parameter  $\varepsilon$ , the dashed line are the exact expression given by (10) and (11).

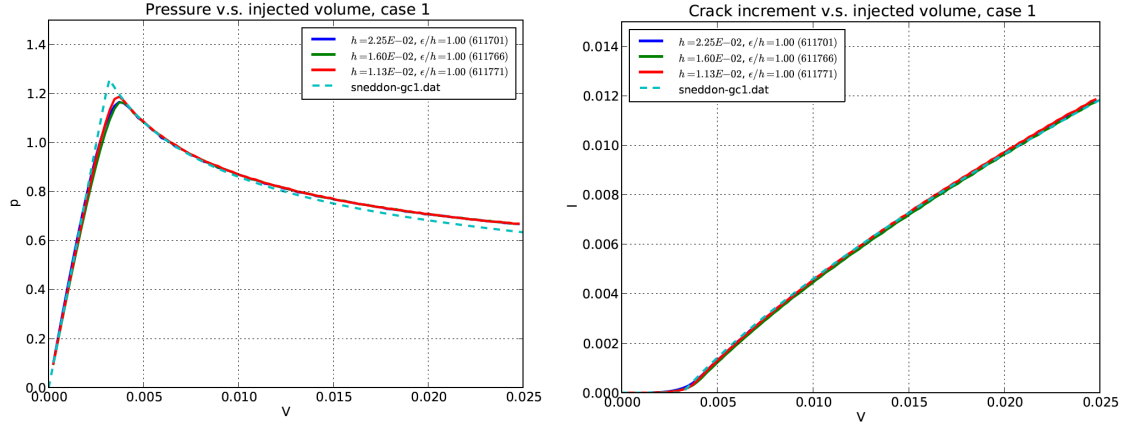


Figure 5: Pressure and length as a function of the injected volume.

and

$$V_0 = \left[ \frac{64R_0^5 G_c \pi}{9E'} \right]^{1/2}. \quad (13)$$

Just as in the two dimensional case, it is possible to show that as long at  $V < V_0$ , the crack does not grow, and that for  $V > V_0$ , the crack radius and pressure are given by

$$p(V) = \left[ \frac{G_c^3 E'^2 \pi^3}{12V} \right]^{1/5}, \quad (14)$$

and

$$R(V) = \left[ \frac{9E'V^2}{64\pi G_c} \right]^{1/5}. \quad (15)$$

We ran a series of three dimensional experiments on a cubic domain  $(0,1) \times (0,1) \times (0,1)$  discretized using various resolution ranging from  $50 \times 50 \times 50$  to  $250 \times 250 \times 250$  finite elements. The Young's modulus



is  $E' = 1$ , the fracture toughness  $G_c = 1.91\text{E-}9$ . We account for a pre-existing penny shape crack of radius  $R_0 = 0.1$  in the plane  $x = 0.5$  by building the  $v$  field given by (8), and prescribe to 0 all components of the displacement field on the boundary of the domain. Figure 6 represents the evolution of the fluid pressure and crack surface area as a function of the injected volume, compared with different resolutions.

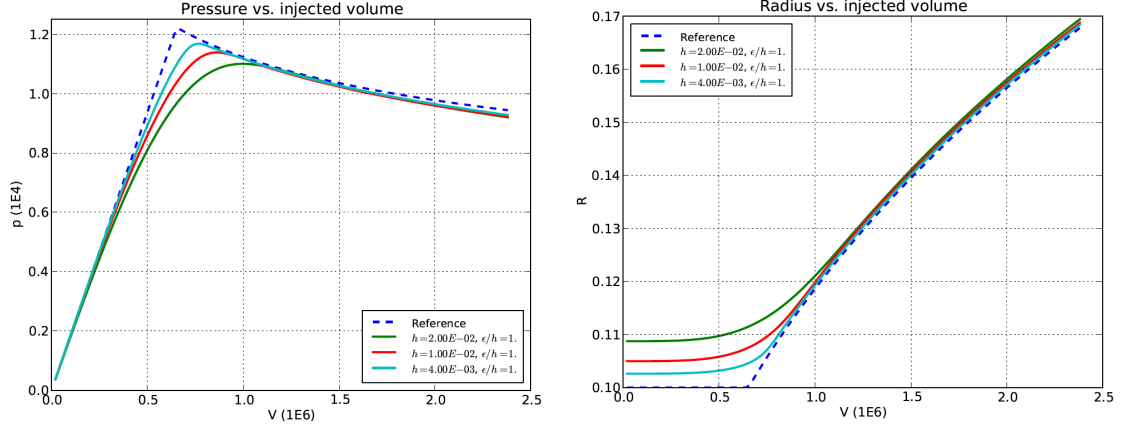


Figure 6: Injection pressure and crack radius as a function of the injected volume. Numerical simulation (solid line) and (14) and (15) (dashed line).

## 5. Interaction between two pressurized cracks in 2d:

The strengths of the variational approach to hydraulic stimulation can be better highlighted in more complicated situations. In a two-dimensional setting, we consider the problem of two pressurized cracks close enough from each other to interact: in a square domain  $\Omega = (0, 8) \times (0, 8)$ , we place two straight cracks of length 1, centered at  $(3, 4.25)$  and  $(4.8, 4.75)$  and with polar angle  $0$  and  $-30^\circ$ . For the sake of simplicity, we only prescribe the total injected volume, and assume that the pressure is constant and equal in each crack.

As the injected volume  $V$  increases, we obtain the following evolution (see Figure 7 for the evolution of the pressure and crack length, and Figure 8 for the evolution of the crack geometry):

1. For  $V < 3.3\text{E-}2$ , the cracks do not propagate and the pressure grows as a linear function of the injected volume.
2. At  $V \simeq 3.3\text{E-}2$ , one of the crack tip activates. A crack grows along a curved path, heading towards the second crack. As expected, crack propagation is accompanied by a fluid pressure drop. The critical pressure is  $p \simeq .66\text{E-}1$ , compared to  $p_0 \simeq .79$  for a single crack.
3. At  $V \simeq 5.6\text{E-}2$ , the cracks connect.
4. From  $V \simeq 5.6\text{E-}2$  until  $V \simeq 6.8\text{E-}2$ , no growth is observed, so that again, the pressure grows linearly;
5. Finally, after  $V \simeq 6.8\text{E-}2$ , another crack tip activates, and we observe again a pressure drop.

We insist that the crack path is not precomputed or enforced through a branching criterion, but is given as a result of energy minimization, and that changes in crack topology are handled transparently by the regularized model. Moreover, handling multiple cracks, or interactions with pre-existing cracks is no more complicated than handling a simple crack.

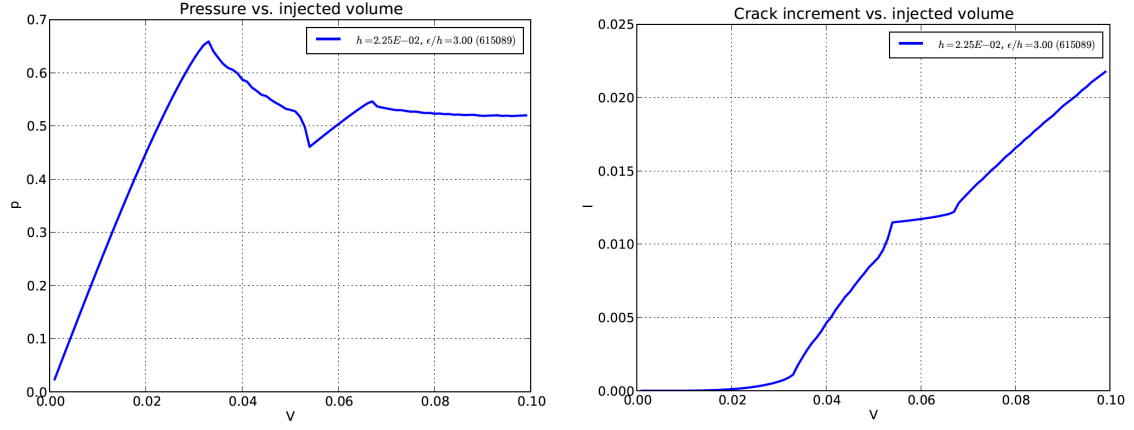


Figure 7: Evolution of the pressure (left) and total crack length (right) for two interacting cracks

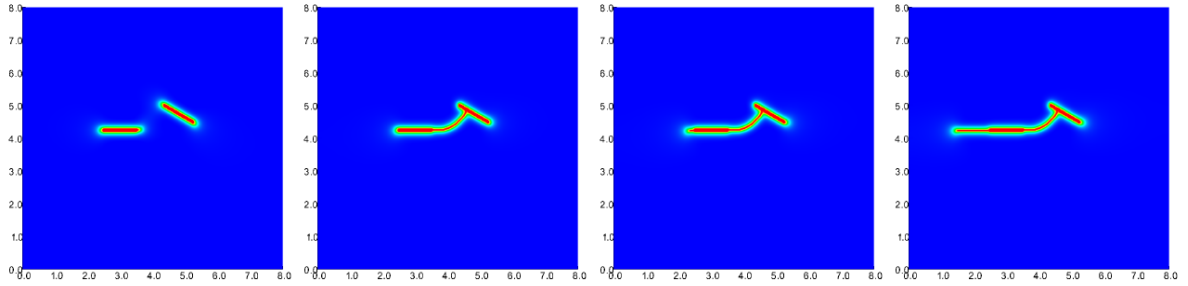


Figure 8: Evolution of the crack geometry. Snapshot of the  $v$  field for an injected volume of .033, .056, .068, and .01.

## 6. Conclusions

We have extended Francfort and Marigo’s variational approach to fracture in order to account for the work of pressure forces occurring during the hydraulic fracturing of reservoirs by fluid injection. The resulting model recasts Griffith’s criterion into a sequence of unilateral minimization problems amongst all possible sets of cracks. It does not require without a priori knowledge of crack geometry, path, or topology, and is applicable in two and three space dimensions. The numerical implementation is based on a regularization similar to a “phase-field” model.

The method was applied to two and three-dimensional problems. In the static case, we obtained values of the crack volume and crack opening displacement along the crack length in good agreement with values calculated from the classical expressions in [22, Sec 2.4]. In the quasi-static setting of prescribed injected volume, we performed qualitative comparison of the evolution of the cracks size and injection pressure with that derived from the aforementioned reference. We illustrated the method’s robustness with respect to mesh size, and effect of the size of the regularization parameter, in two and three dimensions.

Finally, we presented qualitative results of two interacting cracks in a 2d medium, highlighting the capability of the method to handle multiple cracks and their interactions and to predict complex crack path without any additional branching criterion or computational overhead.

This work is the first major step in showing the potential of the variational fracture framework for hydraulic fracturing of petroleum reservoirs. In subsequent works, we intend to couple the fracture model with fluid flow model to capture the essential details relevant in a practical hydraulic fracture application.

## 7. Acknowledgements

We benefited discussing variational fracture simulation with P. Connolly and T. Buchmann of Chevron. We thank Chevron management for permission to publish this work. This material is based in part upon work supported by Chevron under “Variational fracture approach to reservoir stimulation” (C. Chukwudozie and B. Bourdin) and the National Science Foundation under Grants No. DMS-0909267 (B. Bourdin). Some of the numerical experiments were performed using resources from the Extreme Science and Engineering Discovery Environment (XSEDE), supported by National Science Foundation grant number OCI-1053575, and provided by TACC at the University of Texas.

## 8. Nomenclature

$u$	displacement field.
$\Gamma$ :	unknown crack set.
$v$ :	the smooth function representing the crack set $\Gamma$ in (3).
$\Omega$ :	computational domain.
$\mathbf{A}$ :	Hooke’s law.
$e(u)$ :	linearized strain tensor: $e(u) := \frac{\nabla u + \nabla^T u}{2}$ .
$G_c$ :	the fracture toughness.
$\mathcal{H}^{N-1}$ :	the Hausdorff $N - 1$ dimensional measure, i.e. $\mathcal{H}^{N-1}(\Gamma)$ is the length of $\Gamma$ in 2d, and its surface area in 3d.
$p(x)$ :	the pressure of the injected fluid
$\varepsilon$ :	the regularization parameter in (3), homogeneous to a length.
$\ell_0$ :	the length of a preexisting straight crack.
$R_0$ :	the radius of a preexisting penny-shaped crack.

- [1] J. Adachi, E. Siebrits, A. Peirce, and J. Desroches. Computer simulation of hydraulic fractures. *Int. J. Rock Mech. & Min. Sci.*, 44:739–757, 02 2007.

- [2] L. Ambrosio and V.M. Tortorelli. Approximation of functionals depending on jumps by elliptic functionals via  $\Gamma$ -convergence. *Comm. Pure Appl. Math.*, 43(8):999–1036, 1990.
- [3] L. Ambrosio and V.M. Tortorelli. On the approximation of free discontinuity problems. *Boll. Un. Mat. Ital. B (7)*, 6(1):105–123, 1992.
- [4] S. Balay, J. Brown, , K. Buschelman, V. Eijkhout, W.D. Gropp, D. Kaushik, M.G. Knepley, L.C. McInnes, B.F. Smith, and H.Zhang. PETSc users manual. Technical Report ANL-95/11 - Revision 3.3, Argonne National Laboratory, 2012.
- [5] S. Balay, J. Brown, K. Buschelman, W.D. Gropp, D.Kaushik, M.G. Knepley, L.C. McInnes, B.F. Smith, and H. Zhang. PETSc Web page, 2012. <http://www.mcs.anl.gov/petsc>.
- [6] S. Balay, W.D. Gropp, L.C. McInnes, and B.F. Smith. Efficient management of parallelism in object oriented numerical software libraries. In E. Arge, A. M. Bruaset, and H. P. Langtangen, editors, *Modern Software Tools in Scientific Computing*, pages 163–202. Birkhäuser Press, 1997.
- [7] B. Bourdin. Image segmentation with a finite element method. *M2AN Math. Model. Numer. Anal.*, 33(2):229–244, 1999.
- [8] B. Bourdin. Numerical implementation of a variational formulation of quasi-static brittle fracture. *Interfaces Free Bound.*, 9:411–430, 08 2007.
- [9] B. Bourdin, G.A. Francfort, and J.-J. Marigo. Numerical experiments in revisited brittle fracture. *J. Mech. Phys. Solids*, 48(4):797–826, 2000.
- [10] B. Bourdin, G.A. Francfort, and J.-J. Marigo. The variational approach to fracture. *J. Elasticity*, 91(1-3):1–148, 2008.
- [11] A. Braides. *Approximation of Free-Discontinuity Problems*. Number 1694 in Lecture Notes in Mathematics. Springer, 1998.
- [12] A. Chambolle. Finite-differences discretizations of the Mumford-Shah functional. *M2AN Math. Model. Numer. Anal.*, 33(2):261–288, 1999.
- [13] A. Chambolle. An approximation result for special functions with bounded variations. *J. Math Pures Appl.*, 83:929–954, 2004.
- [14] A. Chambolle. Addendum to “An Approximation Result for Special Functions with Bounded Deformation” [J. Math. Pures Appl. (9) 83 (7) (2004) 929–954]: the n-dimensional case. *J. Math Pures Appl.*, 84:137–145, 2005.
- [15] G.A. Francfort and J.-J. Marigo. Revisiting brittle fracture as an energy minimization problem. *J. Mech. Phys. Solids.*, 46(8):1319–1342, 1998.
- [16] H. Gu, J. Weng, J. Lund, U. Mack, M. Ganguly, and R. Suarez-Rivera. Hydraulic fracture crossing natural fracture at nonorthogonal angles: A criterion and its validation. *SPEPO*, SPE 139984:20–26, Feb 2012.
- [17] M.M. Hossain, M.K. Rahman, and S.S. Rahman. Volumetric growth and hydraulic conductivity of naturally fractured reservoirs during hydraulic fracturing: A case study using australian conditions. In *Proceedings of the 2000 SPE Annual Technical Conference and Exhibition*, page SPE 63173, 2000.

- [18] M.J. Mayerhofer, E.P. Lonon, N.R. Warpinski, C.L. Cipolla, D. Walser, and C.M. Rightmire. What is stimulated reservoir volume? *SPEJ*, SPE 119890:89–98, 02 2010.
- [19] Z. Moschovidis, R. Steiger, R. Peterson, N. Warpinski, C. Wright, E. Chesney, J. Hagan, A. Abou-Sayed, R. Keck, M. Frankl, C. Fleming, S. Wolhart, B. McDaniel, A. Sinor, S. Ottesen, L. Miller, R. Beecher, J. Dudley, D. Zinno, and O. Akhmedov. The mounds drill-cuttings injection field experiment: Final results and conclusions. In *Proceeding of the 2000 IADC/SPE Drilling Conference*, SPE 59115, 2000.
- [20] M. Negri. The anisotropy introduced by the mesh in the finite element approximation of the Mumford-Shah functional. *Numer. Funct. Anal. Optim.*, 20(9-10):957–982, 1999.
- [21] J. Rungamornrat, M.F. Wheeler, and M.E. Mear. A numerical technique for simulating nonplanar evolution of hydraulic fractures. In *Proceedings of the 2005 SPE Annual Technical Conference and Exhibition*, page SPE 96968, 2005.
- [22] I.N. Sneddon and M. Lowengrub. *Crack problems in the classical theory of elasticity*. The SIAM series in Applied Mathematics. John Wiley & Sons, 1969.